npg

ORIGINAL ARTICLE

Functional astrocyte–neuron lactate shuttle in a human stem cell-derived neuronal network

Marta A Tarczyluk, David A Nagel, John D O'Neil, H Rheinallt Parri, Erin HY Tse, Michael D Coleman and Eric J Hill

The NT2.D1 cell line is one of the most well-documented embryocarcinoma cell lines, and can be differentiated into neurons and astrocytes. Great focus has also been placed on defining the electrophysiological properties of the neuronal cells, and more recently we have investigated the functional properties of their associated astrocytes. We now show for the first time that human stem cell-derived astrocytes produce glycogen and that co-cultures of these cells demonstrate a functional astrocyte–neuron lactate shuttle (ANLS). The ANLS hypothesis proposes that during neuronal activity, glutamate released into the synaptic cleft is taken up by astrocytes and triggers glucose uptake, which is converted into lactate and released via monocarboxylate transporters for neuronal use. Using mixed cultures of NT2-derived neurons and astrocytes, we have shown that these cells modulate their glucose uptake in response to glutamate. Additionally, we demonstrate that in response to increased neuronal activity and under hypoglycaemic conditions, co-cultures modulate glycogen turnover and increase lactate production. Similar results were also shown after treatment with glutamate, potassium, isoproterenol, and dbcAMP. Together, these results demonstrate for the first time a functional ANLS in a human stem cell-derived co-culture.

INTRODUCTION

Neurons and astrocytes form complex relationships that actively support brain function. Recently, the concept of the tripartite synapse[1] has replaced the traditional neurocentric view of the brain. This hypothesis acknowledges that astrocytes not only conduct housekeeping functions but that they also sense neuronal synaptic transmitter release and in turn can modulate neuronal activity through the release of gliotransmitters.

Astrocytes also have a vital role in neurovascular and neurometabolic coupling.[2] Their anatomic position between blood vessels and neurons make them an ideal interface for effective glucose uptake from blood.[3] They also extend numerous processes that connect via end-feet, blood vessels to the neurons and the extracellular space.[4] Some of these processes ensheath neurons while others are interconnected with other astrocytes via gap junctions to form astrocytic syncitia.[5]

The astrocyte–neuron lactate shuttle hypothesis (ANLS),[6] has profoundly altered our understanding of brain metabolism. The ANLS hypothesis postulates that during neuronal activity, astrocytes respond to glutamatergic activation by increasing glucose utilization, enhancing glycolysis and lactate release.[6] This lactate is then taken up by neurons via MCT2 transporters and is converted to pyruvate for adenosine triphosphate generation by the tricarboxylic acid cycle.[7]

During prolonged activity, astrocytes may also rely upon their reserves of glycogen.[8,9] Glycogenolysis has been shown to be essential in rat hippocampal learning[10] and chick bead discrimination tests.[11]

These metabolic roles in the brain have fundamental implications within the context of stem cell-derived neuronal networks. The NT2.D1 embryocarcinoma cell line is a well-characterized cell line that has been shown to generate both neuronal (NT2.N) and astrocytic (NT2.A) cells.[12,13] The neurophysiological properties of the neuronal cells derived from these cells have been well characterized. Within the NT2.N population, heterogenous subpopulations are produced such as dopaminergic, cholinergic, GABAergic, and glutamatergic neurons.[14–17] NT2.N cells have been found to generate action potentials on depolarization.[18,19] In addition, they also express the high-voltage-activated calcium channels, pharmacologically classified as L, N, P/Q, and R,[20] as well as calcium-activated BK channels, which are involved in neuronal hyperpolarisation after action potential firing.[21] We have recently demonstrated that NT2.D1 cell-derived neuron and astrocyte (NT2.N/A) networks can communicate and so have the potential to interact with each other as observed *in vivo*.[22] If this model is to be applied to the investigation of human neuronal function, it is also essential that the metabolic relationship is sufficiently representative of functional reality.

In this study, we utilized mixed cultures of NT2.N/A cells to investigate the metabolic properties of these cells and measured the response of the astrocytic network to well-characterized neuromodulators. We demonstrate NT2.N/A cells express the main tenets of the ANLS model and display functional characteristics consistent with their neuron–astrocyte metabolic coupling. We also found for the first time that human stem cell-derived astrocytes store glycogen and that neuromodulators such as

glutamate, potassium, and noradrenaline can modulate its turnover. This study establishes that stem cell-derived astrocytes provide metabolic support to their neuronal counterparts, thus demonstrating a tractable human model, which will facilitate the study of the metabolic coupling between neurons and astrocytes and its relationship with CNS functional issues ranging from plasticity to neurodegeneration.

MATERIALS AND METHODS

Cell Culture

Human teratocarcinoma NT2.D1 cells used in this study were kindly donated by Professor Andrews (University of Sheffield, UK). NT2.D1 cells were cultured in Dulbecco's modified Eagle medium high glucose with GlutaMAX, with pyruvate (Invitrogen, Paisley, UK) containing 10% heat-inactivated fetal bovine serum (Invitrogen), 100 units/mL penicillin, and 100 μg/mL streptomycin. NT2.D1 cells were differentiated to produce mixed cultures of neurons and astrocytes using the method described by Woehrling et al.[23] Briefly, after treatment with 10 μmol/L retinoic acid for 4 weeks, NT2 cells were replated at a lower density (1:3) in RA-free medium to separate differentiated cells from undifferentiated cells by sharp striking of the flasks. Cells were then plated into CellBIND 12-well plates (Corning, NY, USA). Subsequently, cells were treated with mitotic inhibitors to suppress the proliferation of non-neural cell types. To supress the growth of undifferentiated cells, cultures were treated with 0.1 μmol/L, cytosine arabinoside for 1 week, followed by 0.1 μmol/L cytosine arabinoside, 3 μmol/L fluorodeoxyuridine, and 5 μmol/L uridine (U) for 4 weeks. All cells were maintained by incubation at 37°C in a humidified atmosphere of 5% CO_2. Unless otherwise stated, all experiments were carried out at 37°C in a humidified atmosphere of 5% CO_2.

Cultures of NT2 astrocytes were isolated from co-cultures according to the method developed by Woehrling et al.[24] NT2.N/A cells were washed ×3 using phosphate-buffered saline (PBS) and then dissociated using Accutase (PAA laboratories, Yeovil, UK). Large NT2.N aggregates settled quickly leaving a single-cell suspension containing astrocytes that were replated into a CellBind 12-well plate. After incubation for 4 hours, any remaining NT2.N cells were washed off the more adherent NT2.A cells using media. All cells were maintained by incubation at 37°C in a humidified atmosphere of 5% CO_2.

Real Time Polymerase Chain Reaction

Total RNA was extracted using Trizol Reagent (Invitrogen), quantified by spectrophotometry, and treated with DNase and an RNase inhibitor (Qiagen, Manchester, UK). One microgram of total RNA was reverse transcribed using the Nanoscript reverse transcriptase kit (Primer Design, Southampton, UK) and oligo dT$_{15}$ primers (Primer Design). Real-time PCR: cDNAs were amplified in a standard 40-cycle SYBR green real-time PCR reaction using optimized sequence specific primers for GLUT1, GLUT3, MCT2, MCT4, MCT1, GLT-1, GLAST, and GLUL according to the manufacturer's instructions. The housekeeping genes UBC, B2M, EIF4A2, and C14orf133 (supplied by Primer Design) were assayed under the same conditions as above. The expression of UBC was found to be unchanged under the conditions imposed and was therefore used in the normalization of qRT-CR data. Cycling conditions were as follows: 10 minutes at 95°C, 15 seconds at 95°C, and 1 minute at 60°C for 40 cycles, 30 seconds at 95°C, 30 seconds at 55°C, and 30 seconds at 95°C. The following formula was used to calculate the relative amount of the transcripts in differentiated (treat) and the undifferentiated samples (control), both of which were normalized to the endogenous controls. $\Delta\Delta CT = \Delta CT$ (treat)—ΔCT (control) for biologic RNA samples or $\Delta\Delta CT = \Delta CT$ (HBRR) – ΔCT (UHRR) for reference RNA samples. ΔCT is the difference in CT between the target gene and endogenous controls by subtracting the average CT of controls from each replicate. The fold change for each treated sample (relative to the control sample (or UHRR) = $2^{-\Delta\Delta CT}$. Fold changes in gene expression using the comparative CT method and statistical analysis were determined using the freely available Relative Expression Software Tool (REST 2009, http://www.qiagen.com). Fold changes > 2 fold were considered significant.

Immunohistochemistry

Cells cultured on PDL/Laminin coverslips (BD Biosciences, Oxford, UK) were washed with PBS and fixed for 10 minutes with 4% paraformaldehyde. After fixation, coverslips were washed twice with PBS and permeabilized with 0.2% Triton/PBS. Subsequently, cells were incubated in 2% BSA/0.2% Triton/PBS for 1 hour to avoid non-specific binding of antibody. Subsequently, cells were incubated for 1 hour at room temperature with either mouse anti-glial fibrillary acidic protein (clone GA5 Millipore, Watford, UK, 1:500) or rabbit anti- β-tubulin-III (Abcam, Cambridge, UK, 1:500). After incubation, coverslips were washed three times in 2% BSA/0.2% Triton/PBS and then incubated with donkey anti-mouse Rhodamine (1:200, Jackson ImmunoResearch, Suffolk, UK) and goat anti-rabbit FITC (1:200; Jackson Immunoresearch).

After washing, the nuclei were visualized by Hoechst staining (Invitrogen) and mounted with ProLong Gold Antifade Reagent (Invitrogen). The cells were examined using a Leica DM14000 B (Leica Microsystems, Milton, Keynes, UK).

Glycogen Staining

Cytologic localization of glycogen was determined using the periodic acid-Schiff method.[25] Briefly, the cells cultured on coverslips were washed with
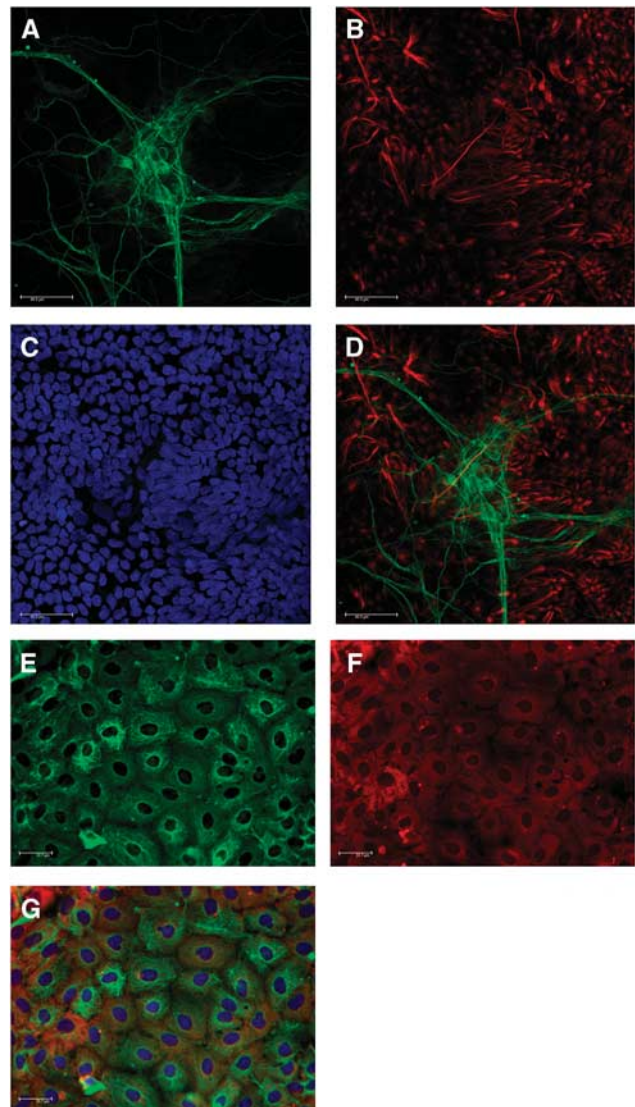

Figure 1. Immunofluorescent image of NT2.N/A. Images showing (**A**) β-tubulin positive NT2.N (green), (**B**) glial fibrillary acidic protein (GFAP)-positive NT2.A (red), (**C**) Nuclei stained with Hoechst and (**D**) overlay of GFAP-positive astrocytes and β-tubulin-positive neurons. (**E**) Immunostaining of astrocytes (green) and (**F**) staining for glycogen (red) using the periodic acid-Schiff assay. (**G**) Representative image of co-localization of glycogen and GFAP (yellow), Hoechst (Blue). No glycogen staining was observed in NT2.N. Scale bar 40 and 33.7 μmol/L.

ice-cold PBS and fixed for 5 minutes at room temperature in methanol. After fixation, coverslips were washed three times with 70% (vol/vol) ethanol. Subsequently, the cells were incubated for 30 minutes at room temperature with 1% (wt/vol) periodic acid dissolved in 70% ethanol. After incubation, cells were washed three times with 70% ethanol and stained for 60 minutes at room temperature with 0.5% (wt/vol) basic fuchsin (Sigma-Aldrich, Dorset, UK) dissolved in acid ethanol (ethanol/water/ concentrated HCl, 80:19:1). Finally, cells were washed three times with 70% ethanol.

Determination of Glycogen Levels

The method used to determine levels of glycogen in biologic samples was first described in.[26] After the treatment, cells were washed three times with ice-cold PBS and then scraped in 300 μl of 30 mmol/L ice-cold HCl. Subsequently, samples were sonicated for 15 seconds and both glycogen and protein content was determination. Ten microliter aliquots of cell lysate were sampled. To the first aliquot, 30 μl of acetate buffer (0.1 mol/L, pH 4.65) was added. To the second 30 μl of 0.1 mg/mL of amyloglucosidase in acetate buffer was added. Both samples were incubated for 30 minutes at room temperature. After incubation, 200 μL of Tris-HCl buffer (0.1 mol/L, pH 8.1) containing MgCl$_2$ (3.3 mmol/L), adenosine triphosphate (0.33 mmol/L), nicotinamide adenine dinucleotide phosphate (38 μmol/L), hexokinase (4 μg/mL), and glucose 6-phosphate dehydrogenase (2 μg/mL) were added to both aliquots and incubated for 30 minutes at room temperature. Standards were prepared using a solution of glucose (1 mg/ mL) and 1:2 serially diluted using acetate buffer to provide standards ranging from 500 μg/ml and 3.9 μg/ml. Standards were incubated with acetate buffer for 30 minutes at room temperature and then with hexokinase and glucose 6-phosphate dehydrogenase for 30 minutes at room temperature. Fluorescence of the NADPH formed in the final reaction (excitation: 340 nm; emission: 450 nm) was obtained using SpectraMAX GeminiXS microplate luminometer (Molecular Devices, Berkshire, UK) and SoftMaxPro software. The first aliquot provides the sum of glucose and glucose 6-phosphate, and the second corresponds to total NADPH derived from glycogen, glucose, and glucose 6-phosphate. One mole of glycogen corresponds to 1 mol of glycosyl units originating from glycogen. The remaining 10 μl sample was used to determine protein content using BCA assay reagent kit from (Thermofisher, Loughborough, UK) and read at 590 nm using a Thermo multiscan EX 96 well plate reader (Thermofisher).

6-NBDG Uptake Assay

Uptake of the glucose analog 6-NBDG (Invitrogen) in NT2.N/A and NT2.A cultures was investigated using methods described by Waiza et al.[27] Briefly, before measurement, culture medium was removed and the cells were washed with Krebs–Ringer HEPES buffer supplemented with 5 mmol/L glucose. Glucose in the medium was reduced to 0.5 mmol/L and the cells were incubated for 5 minutes. Subsequently, the buffer in each well was replaced with Krebs–Ringer HEPES buffer containing 0.5 mmol/L glucose and 300 μmol/L 6-NBDG. Cultures were excited at 488 nm and imaged at 505 to 550 nm emission at 60 minutes, 180 minutes, and 360 minutes. Absorbance was measured using SpectraMAX GeminiXS microplate luminometer (Molecular Devices).

Determination of Lactate Levels

Lactate was measured using the Fluorescent Lactate Assay Kit (Abcam). Briefly, the assay was carried out in a 96 well microplate. Fifty microlitersof media samples were used and well mixed with 50 μl reaction mix containing 46 μl lactate assay buffer, 2 μl probe, and 2 μl enzyme mix. Fifty microliters of lactate standards prepared at 0, 0.2, 0.4, 0.6, 0.8, and 1.0 nmol/well and 50 μl reaction mix. The reaction was incubated at room temperature for 30 minutes (protected from light) and absorbance at 570 nm was obtained using a Thermo multiscan EX 96 well plate reader. All readings were corrected for background.
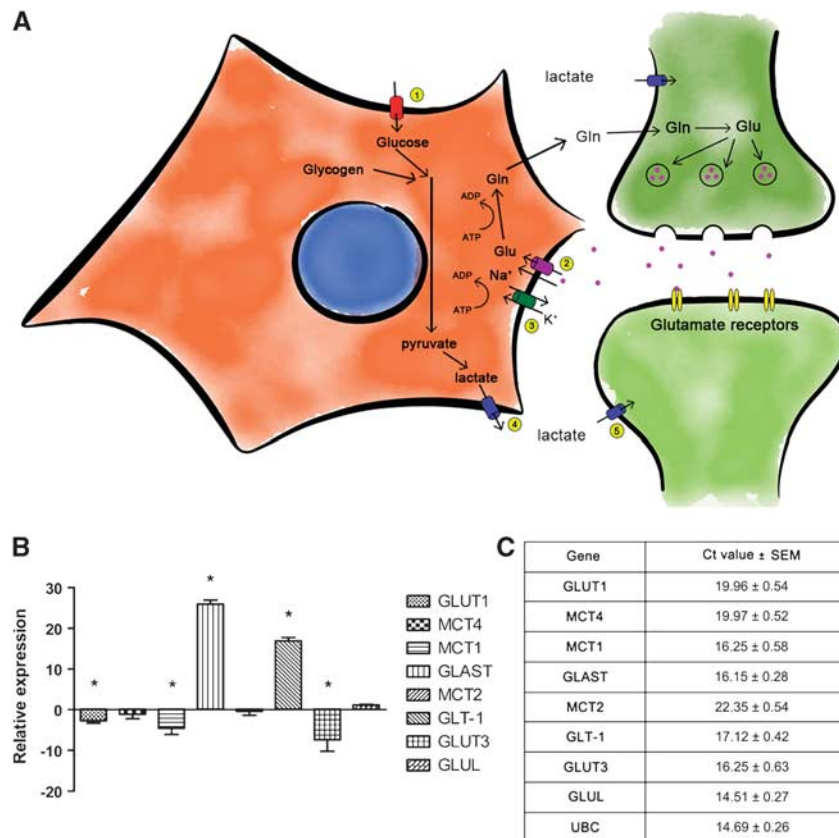

Figure 2. Characterization of ANLS components in NT2.N/A after differentiation. (**A**) Schematic diagram of the astrocyte–neuron lactate shuttle (ANLS). 1 = GLUT1; 2 = GLAST/GLT-1; 3 = Na + /K + ATPase; 4 = MCT1/4; 5 = MCT2. (**B**) mRNA expression of GLUT1, GLUT3, MCT2, MCT4, MCT1, GLT-1, GLAST, and GLUL, as well the housekeeping gene, UBC, expressed as the average fold change ± s.e.m. (*n* = 3) and (**C**) Ct values ± s.e.m. (*n* = 3).

Gene	Ct value ± SEM
GLUT1	19.96 ± 0.54
MCT4	19.97 ± 0.52
MCT1	16.25 ± 0.58
GLAST	16.15 ± 0.28
MCT2	22.35 ± 0.54
GLT-1	17.12 ± 0.42
GLUT3	16.25 ± 0.63
GLUL	14.51 ± 0.27
UBC	14.69 ± 0.26

Stimulation Protocol

NT2.D1 cultures were synaptically stimulated using a computer controlled constant current isolated -stimulator (STG1002, Multichannel Systems, Reutligen, Germany) and bipolar electrodes, which were placed within close proximity to cells.

Statistics

Results were expressed as the mean of three samples ± s.e. of the mean. Comparisons between treatments were performed using analysis of variance followed by Dunnett's or Turkey's post test or Student's t-test using GraphPad Prism Software (La Jolla, CA, USA). Differences were considered significant for P values < 0.05.

RESULTS

NT2.D1-derived neurons (NT2.N) and astrocytes (NT2.A) were identified visually by their characteristic morphology. NT2.A cells were identified by their flat phase dark appearance, while NT2.Ns were typically phase bright and often observed on top of the astrocytic monolayer. These cells were further identified using immunohistochemistry for the specific markers glial fibrillary acidic protein and β-tubulin (Figure 1). To determine the localization of glycogen in NT2.D1-derived cultures, the periodic acid – Schiff method was used.[26] Glycogen was found to co-localize with glial fibrillary acidic protein-positive cells (Figure 1G).

Using real-time qRT-PCR, cultures were also characterized for the expression of genes involved in the ANLS after differentiation. Genes included glucose transporters (GLUT1 and GLUT3), monocarboxylate transporters (MCT1, MCT2, and MCT4), glutamate transporters (GLT1 and GLAST) and glutamine synthase (GLUL). A comparison of undifferentiated NT2.D1 cells with differentiated co-cultures showed an upregulation of glutamate transporters (GLAST and GLT1) and a downregulation of GLUT1, MCT1, and GLUT3, while other genes remained unchanged (MCT4/2 and GLUL); (Figure 2B). However, Ct values for all genes tested were relatively low (< 30) suggesting a high-to-moderate expression of these genes (Figure 2C).

Glutamate Stimulates Uptake of Fluorescent Glucose Analog 6-NBDG in NT2.N/A Cultures

Utilization of glucose in NT2.N/A and NT2.A cultures was monitored using the fluorescent glucose analog 6-NBDG. In control, cultures dye accumulated 1.68-fold ± 0.165 s.e.m. over 360 minutes from 0 minute. After the treatment of the cultures with glutamate for 180 minutes, 6-NBDG uptake in co-cultures increased 2.09 fold ± 0.144 s.e.m. ($P < 0.01$) (Figure 3A). The uptake of 6-NBDG induced by glutamate was completely blocked by ouabain, a Na$^+$/K$^+$ ATPase inhibitor. Similarly, treatment with cytochalasin B, a potent inhibitor of GLUT1 and GLUT4-mediated glucose uptake, blocked the uptake of 6-NBDG. Similar results were also obtained in pure NT2.A cultures (Figure 3B).

Hypoglycemic and Neuromodulators Stimulate Turnover of Glycogen and Production of Lactate

Lactate release and glycogen levels were measured in KREBS-ringer HEPES buffer containing no glucose. In order to block
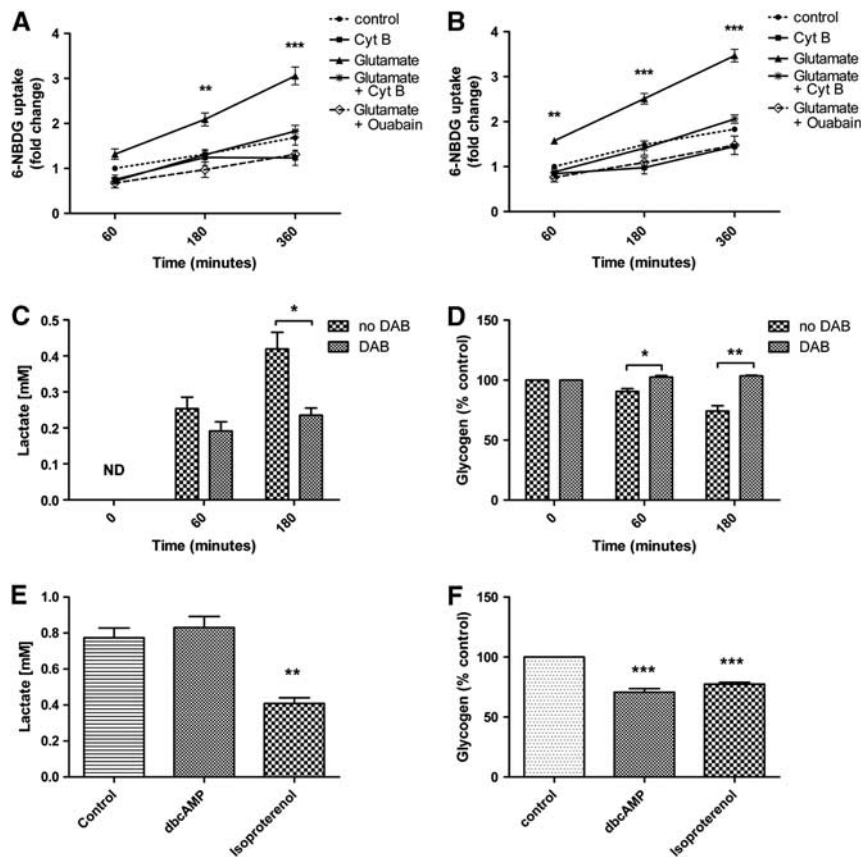

Figure 3. Effects of glutamate, hypoglycemia, and neuromodulators on 6-NBDG uptake, lactate production, and glycogen breakdown in NT2.D1-derived cultures. Uptake was measured in the presence of glutamate with and without ouabain or cytochalasin B in, (**A**) NT2.N/A, (**B**) pure NT2.A culture, (**C**) lactate production under hypoglycaemic conditions (ND, non detected), (**D**) glycogen turnover under hypoglycemic conditions, (**E**) lactate production in cells treated with dbcAMP and isoproterenol for 180 minutes, (**F**) glycogen turnover in cells treated with dbcAMP and isoproterenol for 180 minutes. Results are expressed as the mean ± s.e.m. ($n = 3$). $P < 0.05$ (*), $P < 0.01$ (**), $P < 0.001$ (***).

glycogen breakdown, cells were also treated with 1,4-dideoxy-1,4-imino-d-arabinitol, a selective inhibitor of glycogen phosphorylase. Under hypoglycaemic conditions (Figure 3C), cultures released significant amounts of lactate (0.42 ± 0.05 mmol/L at 180 minutes, $P < 0.001$) as well as degrading glycogen to $90.62 \pm 2.33\%$ at 60 minutes and $74.23 \pm 4.48\%$ at 180 minutes, ($P < 0.01$; Figure 3D) of the control. 1,4-dideoxy-1,4-arabinitol treatment significantly decreased the release of lactate (180 minutes, $P < 0.05$) as well as the breakdown of glycogen

(180 minutes, $P < 0.01$). Treatments with known modulators of glycogen phosphorylase, dbcAMP as well as the β_1 and β_2 adrenergic agonist isoproterenol induced a significant decrease in glycogen levels in comparison with non-treated control ($P < 0.001$) (Figure 4F). In comparison, lactate levels after exposure to dbcAMP did not show any significant increase while isoproterenol treatment resulted in a significant decrease in lactate levels to 0.42 ± 0.03 mmol/L, ($P < 0.01$) when compared with the control at 0.77 ± 0.05 mmol/L (Figure 4E).
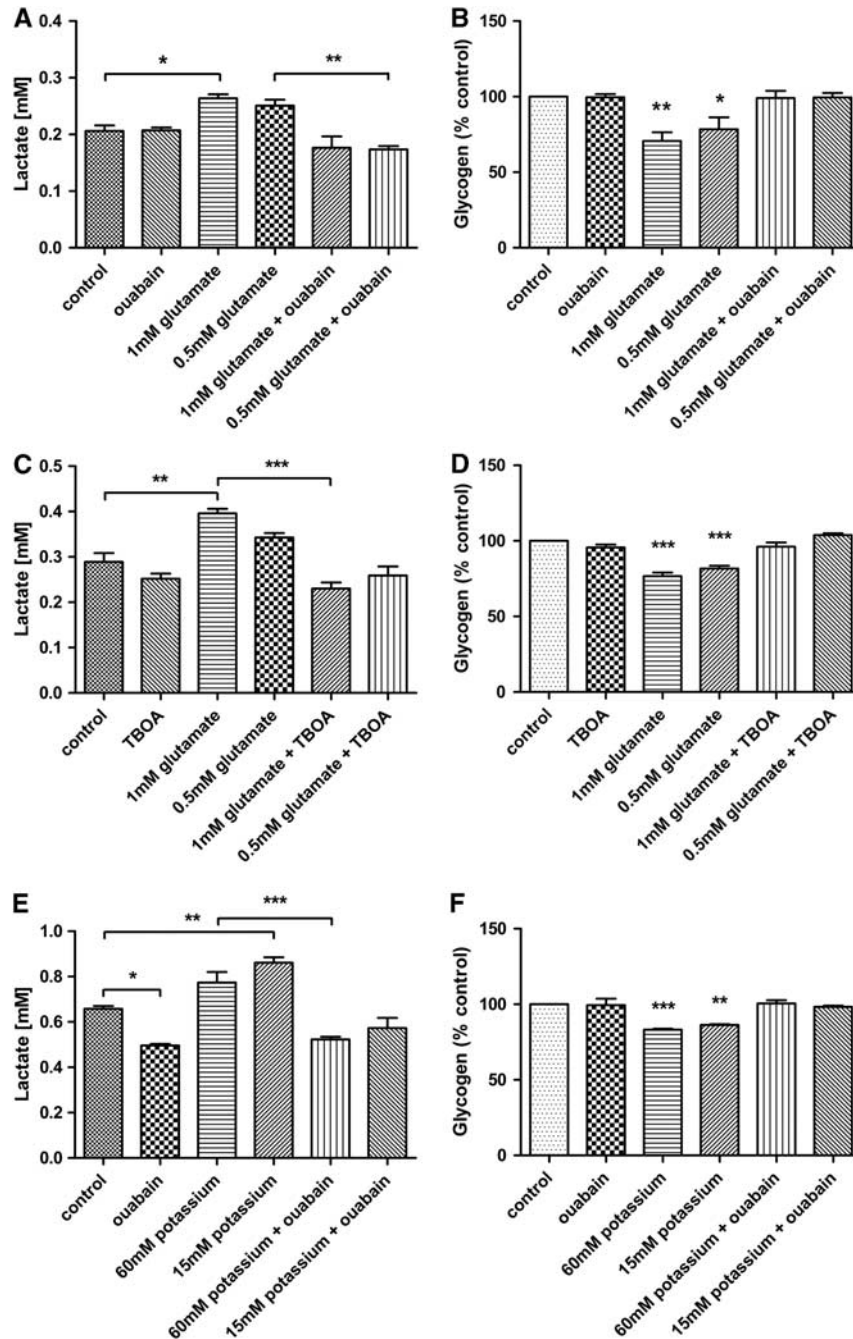

Figure 4. Effects of glutamate and potassium on neuron and astrocytes co-cultures. (**A**) Lactate production in response to glutamate in the presence/absence of ouabain. (**B**) Glycogen turnover in response to glutamate in the presence/absence of ouabain. (**C**) Lactate production in response to glutamate in the presence/absence of DL-*threo*-β-benzyloxyaspartic acid (TBOA). (**D**) Glycogen turnover in response to glutamate in the presence/absence of TBOA. (**E**) Lactate production in response to potassium in the presence/absence of ouabain. (**F**) Glycogen turnover in response to potassium and in the presence/absence of ouabain. Results are expressed as the mean ± s.e.m. ($n = 3$). $P < 0.05$ (*), $P < 0.01$ (**), $P < 0.001$ (***).

Glutamate and Potassium Stimulate Glycogen Breakdown and Lactate Production in NT2.N/A Co-Cultures

In order to test activation of the Na^+/K^+ ATPase by glutamate, cultures were exposed to glutamate both in the presence and absence of ouabain (Figures 4A and 4B). The treatment of the cultures with glutamate significantly increased the lactate levels (1 mmol/L glutamate: 0.26 ± 0.01 mmol/L, $P < 0.05$). Incubation with both glutamate and ouabain reduced the release of lactate back to control levels (control: 0.21 ± 0.01 mmol/L, ouabain and 0.5 mmol/L glutamate: 0.17 ± 0.01 mmol/L) (Figure 4A). In addition, treatment with glutamate caused a significant breakdown of glycogen (1 mmol/L glutamate: 76.75 ± 2.36, $P < 0.01$; 0.5 mmol/L glutamate: $81.73 \pm 1.82\%$, $P < 0.05$). This effect was completely blocked by ouabain (Figure 4B).

To determine whether the effect seen in NT2.N/A cultures was mediated by glutamate transporters and not glutamate receptors,[6] cells were exposed to glutamate in the presence of DL-threo-β-benzyloxyaspartic acid (TBOA), a potent glutamate transport inhibitor. Results demonstrated that TBOA treatment blocks both the release of lactate (control: 0.29 ± 0.02 mmol/L, TBOA and 1 mmol/L glutamate: 0.23 ± 0.01 mmol/L) as well as glycogen breakdown in response to glutamate (TBOA and 1 mmol/L glutamate: $96.16 \pm 2.83\%$ of non-treated control) (Figures 4C and 4D).

Potassium has also been shown to directly activate the Na^+/K^+ ATPase.[28] The levels of lactate after treatment with ouabain alone actually decreased, suggesting a block of basal Na^+/K^+ ATPase activity (Figure 4E). Treatment with potassium at both 15 and 60 mmol/L triggered a significant increase in lactate (60 mmol/L potassium: 0.77 ± 0.05 mmol/L, $P < 0.001$, 15 mmol/L potassium: 0.86 ± 0.02 mmol/L, $P < 0.01$). This effect was completely inhibited in the presence of ouabain (Figure 4E). In addition, glycogen levels were significantly reduced after treatment with potassium (60 mmol/L potassium: $83.25 \pm 0.62\%$, $P < 0.001$, 15 mmol/L potassium: $86.28 \pm 0.54\%$, $P < 0.01$). This effect was again completely blocked with ouabain (Figure 4F).

NT2.N/A Network Activity Induces Glycogen Turnover and Lactate Production

In order to test whether neuronal activity triggers the lactate shuttle in NT2.N/A cultures, the cells were stimulated electrically for 30 minutes using a computer controlled constant current isolated stimulator and bipolar electrodes in the presence and absence of TBOA (Figure 5). After electrical stimulation, the levels of lactate in the media were significantly increased (0.67 ± 0.04 mmol/L $P < 0.01$) in comparison to control (0.36 ± 0.03 mmol/L) (Figure 5C). In addition, glycogen levels inside the cells were significantly decreased ($77.98 \pm 3.62\%$ of the non-stimulated control $P < 0.01$) (Figure 5E). These effects were completely blocked after treatment with TBOA (Figures 5D and 5E). Experiments were carried out at 37°C.

DISCUSSION

The ANLS was first proposed by Pellerin and Magistretti[6] and has since been extensively studied. Experiments supporting the ANLS have been carried out using brain slices, cultured primary neurons, and astrocytes as well as isolated nerves and sympathetic ganglia from rat, mouse, and chick.[29] In addition, a number of studies have used ^{13}C-NMR spectroscopy to comprehensibly investigate cerebral metabolism both in vivo and in vitro.[30,31] However, to date, no studies have determined the existence of the ANLS in human stem cell-derived cultures.

We have previously demonstrated that neuronal networks derived from NT2.D1 cells signal to astrocytes, and that astrocytic networks communicate via gap junction-mediated and gliotransmitter signaling.[22] We now demonstrate for the first time that human stem cell-derived astrocytes synthesize glycogen as well as markers associated with its metabolism, suggesting that these cells are well differentiated and resemble mature astrocytes.[32] Co-cultures also respond to neuromodulators and neuronal activity by enhancing glucose uptake as well as inducing glycogenesis and glycogenolysis. While postmitotic co-cultures derived from NT2.D1 cells are widely accepted as a model of the human CNS, some studies have suggested that NT2.NA resemble human fetal primary cells.[33] As such, caution in the interpretation of NT2-derived cultures to adult cells should be taken.

Our results support the hypothesis that astrocytes respond to glutamate and potassium, by inducing glucose uptake and aerobic glycolysis, resulting in lactate production via activation of Na^+/K^+ ATPase (an effect that was blocked by cytochalasin B, TBOA, and ouabain). We also demonstrate that lactate production and glycogen breakdown occur in astrocytes after neuronal
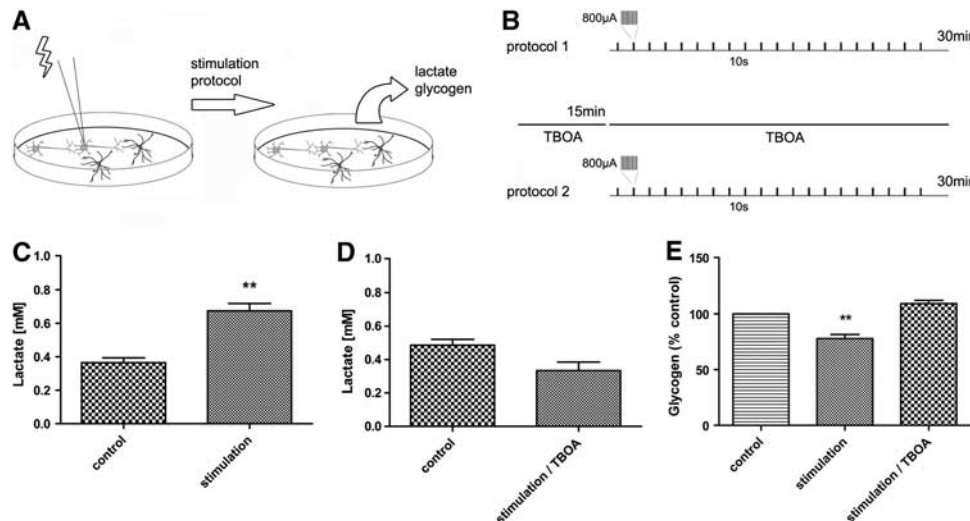

Figure 5. Effects of induced NT2.N/A network activity on glycogen turnover and lactate production. (**A**, **B**) Schematic diagram of the experiment and protocols for electrical stimulation. Production of lactate (**C**, **D**) and breakdown of glycogen (**E**) were measured in response to high-frequency electrical activity in the presence and absence of DL-threo-β-benzyloxyaspartic acid (TBOA). Results are expressed as the mean $\pm$ s.e.m. ($n = 3$). $P < 0.05$ (*), $P < 0.01$ (**), $P < 0.001$ (***).

activation and hypoglycemia and is blocked using 1,4-dideoxy-1,4-imino-d-arabinitol.[34–37]

These results, together with glycogen staining, suggest that NT2.A cells possess the machinery required for glycogen synthesis and glycogen breakdown. The decrease in glycogen levels and subsequent increase in lactate suggest that NT2.A respond to glutamate and potassium, not only by increasing glucose uptake, but also by degrading glycogen as demonstrated in vivo and in primary cultures.[34–36,38]

Treatments of co-cultures with dbcAMP and the β_1 and β_2-adrenoreceptor agonist isoproterenol-induced glycogenolysis within astrocytes. dbcAMP activates glycogen phosphorylase through activation of protein kinase A leading to glycogen breakdown[39] while isoproterenol in turn acts by elevating levels of cyclic AMP.[40] Interestingly, although isoproterenol increased glycogen turnover in these cultures, there was a decrease in the level of lactate in the media. However, it has previously been shown that norepinephrine enhances the expression of MCT2 and subsequent lactate uptake in cortical neurons.[41]

The effect of neuronal activity on glycolysis and glycogenolysis was also investigated using electrical stimulation. After 30 minutes, glycogen levels dropped significantly, while lactate levels increased. Stimulation-induced glycogen breakdown and lactate release were inhibited by TBOA suggesting that neuronal glutamate release and subsequent astrocytic uptake directly induced glycolysis and glycogeneolysis in these cultures.

While the majority of lactate produced in these co-cultures is predicted to be derived from astrocytes, it cannot be unambiguously proved that neurons do not produce lactate in these cultures. As such, future experiments will aim to determine metabolic flux from both cell types in monocultures. In addition, more sensitive methods such as ^{13}C-NMR flux analysis could be used to comprehensively analyze energy metabolism in these cultures.

Glycolysis and glycogenolysis are important processes in normal functioning of the brain but also in a number of disease processes such as ischemia, hypoglycemia, and Alzheimer's. The focus of this report demonstrates the metabolic coupling of neurons and astrocytes for the first time in a human-derived stem cell model. This has important implications in the study of memory formation, plasticity, and neurodegeneration in vitro. In addition, this model may facilitate the future study of the active contribution of astrocytes to the activity of neuronal networks in vitro and indeed, in other basic aspects of human brain function.

DISCLOSURE/CONFLICT OF INTEREST

The authors declare no conflict of interests.

REFERENCES

1 Volterra A, Meldolesi J. Astrocytes, from brain glue to communication elements: the revolution continues. Nat Rev Neurosci 2005; 6: 626–640.

2 Allaman I, Belanger M, Magistretti PJ. Astrocyte-neuron metabolic relationships: for better and for worse. Trends Neurosci 2011; 34: 76–87.

3 Gordon GR, Mulligan SJ, MacVicar BA. Astrocyte control of the cerebrovasculature. Glia 2007; 55: 1214–1221.

4 Kacem K, Lacombe P, Seylaz J, Bonvento G. Structural organization of the perivascular astrocyte endfeet and their relationship with the endothelial glucose transporter: a confocal microscopy study. Glia 1998; 23: 1–10.

5 Giaume C, Koulakoff A, Roux L, Holcman D, Rouach N. Astroglial networks: a step further in neuroglial and gliovascular interactions. Nat Rev Neurosci 2010; 11: 87–99.

6 Pellerin L, Magistretti PJ. Glutamate uptake into astrocytes stimulates aerobic glycolysis: a mechanism coupling neuronal activity to glucose utilization. Proc Natl Acad Sci USA 1994; 91: 10625–10629.

7 Pellerin L, Magistretti PJ. Sweet sixteen for ANLS. J Cereb Blood Flow Metab 2012; 32: 1152–1166.

8 Obel LF, Muller MS, Walls AB, Sickmann HM, Bak LK, Waagepetersen HS et al. Brain glycogen–new perspectives on its metabolic function and regulation at the subcellular level. Front Neuroenergetics 2012; 4: 3.

9 Dienel GA, Wang RY, Cruz NF. Generalized sensory stimulation of conscious rats increases labeling of oxidative pathways of glucose metabolism when the brain glucose-oxygen uptake ratio rises. J Cereb Blood Flow Metab 2002; 22: 1490–1502.

10 Suzuki A, Stern SA, Bozdagi O, Huntley GW, Walker RH, Magistretti PJ et al. Astrocyte-neuron lactate transport is required for long-term memory formation. Cell 2011; 144: 810–823.

11 Gibbs ME, Anderson DG, Hertz L. Inhibition of glycogenolysis in astrocytes interrupts memory consolidation in young chickens. Glia 2006; 54: 214–222.

12 Andrews PW. Retinoic acid induces neuronal differentiation of a cloned human embryonal carcinoma cell line in vitro. Dev Biol 1984; 103: 285–293.

13 Sandhu JK, Sikorska M, Walker PR. Characterization of astrocytes derived from human NTera-2/D1 embryonal carcinoma cells. J Neurosci Res 2002; 68: 604–614.

14 Sodja C, Fang H, Dasgupta T, Ribecco M, Walker PR, Sikorska M. Identification of functional dopamine receptors in human teratocarcinoma NT2 cells. Brain Res Mol Brain Res 2002; 99: 83–91.

15 Newman MB, Kuo YP, Lukas RJ, Sanberg PR, Douglas Shytle R, McGrogan MP et al. Nicotinic acetylcholine receptors on NT2 precursor cells and hNT (NT2-N) neurons. Brain Res Dev Brain Res 2002; 139: 73–86.

16 Garcia de Arriba S, Wegner F, Gruner K, Verdaguer E, Pallas M, Camins A et al. Different capacities of various NMDA receptor antagonists to prevent ischemia-induced neurodegeneration in human cultured NT2 neurons. Neurochem Int 2006; 49: 466–474.

17 Neelands TR, Zhang J, Macdonald RL. GABA(A) receptors expressed in un-differentiated human teratocarcinoma NT2 cells differ from those expressed by differentiated NT2-N cells. J Neurosci 1999; 19: 7057–7065.

18 Hartley RS, Margulis M, Fishman PS, Lee VM, Tang CM. Functional synapses are formed between human NTera2 (NT2N, hNT) neurons grown on astrocytes. J Comp Neurol 1999; 407: 1–10.

19 Coyle DE, Li J, Baccei M. Regional differentiation of retinoic acid-induced human pluripotent embryonic carcinoma stem cell neurons. PLoS One 2011; 6: e16174.

20 Neelands TR, King AP, Macdonald RL. Functional expression of L-, N-, P/Q-, and R-type calcium channels in the human NT2-N cell line. J Neurophysiol 2000; 84: 2933–2944.

21 Chapman H, Piggot C, Andrews PW, Wann KT. Characterisation of large-conductance calcium-activated potassium channels (BK(Ca)) in human NT2-N cells. Brain Res 2007; 1129: 15–25.

22 Hill EJ, Jimenez-Gonzalez C, Tarczyluk M, Nagel DA, Coleman MD, Parri HR. NT2 derived neuronal and astrocytic network signalling. PLoS One 2012; 7: e36098.

23 Woehrling EK, Hill EJ, Coleman MD. Development of a neurotoxicity test-system, using human post-mitotic, astrocytic and neuronal cell lines in co-culture. Toxicol In Vitro 2007; 21: 1241–1246.

24 Woehrling EK, Hill EJ, Coleman MD. Evaluation of the importance of astrocytes when screening for acute toxicity in neuronal cell systems. Neurotox Res 2010; 17: 103–113.

25 Rosenberg PA, Dichter MA. Glycogen accumulation in rat cerebral cortex in dissociated cell culture. J Neurosci Methods 1985; 15: 101–112.

26 Nahorski SR, Rogers KJ. An enzymic fluorometric micro method for determination of glycogen. Anal Biochem 1972; 49: 492–497.

27 Loaiza A, Porras OH, Barros LF. Glutamate triggers rapid glucose transport stimulation in astrocytes as evidenced by real-time confocal microscopy. J Neurosci 2003; 23: 7337–7342.

28 Bittner CX, Valdebenito R, Ruminot I, Loaiza A, Larenas V, Sotelo-Hitschfeld T et al. Fast and reversible stimulation of astrocytic glycolysis by K + and a delayed and persistent effect of glutamate. J Neurosci 2011; 31: 4709–4713.

29 Pellerin L. Lactate as a pivotal element in neuron–glia metabolic cooperation. Neurochem Int 2003; 43: 331–338.

30 Amaral AI, Teixeira AP, Hakonsen BI, Sonnewald U, Alves PM. A comprehensive metabolic profile of cultured astrocytes using isotopic transient metabolic flux analysis and C-labeled glucose. Front Neuroenergetics 2011; 3: 5.

31 Zwingmann C, Leibfritz D. Regulation of glial metabolism studied by 13C-NMR. NMR Biomed 2003; 16: 370–399.

32 Brunet JF, Allaman I, Magistretti PJ, Pellerin L. Glycogen metabolism as a marker of astrocyte differentiation. J Cereb Blood Flow Metab 2010; 30: 51–55.

33 Goodfellow CE, Graham SE, Dragunow M, Glass M. Characterization of NTera2/D1 cells as a model system for the investigation of cannabinoid function in human neurons and astrocytes. J Neurosci Res 2011; 89: 1685–1697.

34 Swanson RA, Morton MM, Sagar SM, Sharp FR. Sensory stimulation induces local cerebral glycogenolysis: demonstration by autoradiography. Neuroscience 1992; 51: 451–461.

35 Swanson RA. Physiologic coupling of glial glycogen metabolism to neuronal activity in brain. Can J Physiol Pharmacol 1992; 70(Suppl): S138–S144.

36 Cruz NF, Dienel GA. High glycogen levels in brains of rats with minimal environmental stimuli: implications for metabolic contributions of working astrocytes. *J Cereb Blood Flow Metab* 2002; **22**: 1476–1489.

37 Walls AB, Sickmann HM, Brown A, Bouman SD, Ransom B, Schousboe A et al. Characterization of 1,4-dideoxy-1,4-imino-d-arabinitol (DAB) as an inhibitor of brain glycogen shunt activity. *J Neurochem* 2008; **105**: 1462–1470.

38 Hof PR, Pascale E, Magistretti PJ. K+ at concentrations reached in the extracellular space during neuronal activity promotes a Ca2+-dependent glycogen hydrolysis in mouse cerebral cortex. *J Neurosci* 1988; **8**: 1922–1928.

39 Boer P, Sperling O. Modulation of glycogen phosphorylase activity affects 5-phosphoribosyl-1-pyrophosphate availability in rat hepatocyte cultures. *Nucleosides Nucleotides Nucleic Acids* 2004; **23**: 1235–1239.

40 Sorg O, Magistretti PJ. Vasoactive intestinal peptide and noradrenaline exert long-term control on glycogen levels in astrocytes: blockade by protein synthesis inhibition. *J Neurosci* 1992; **12**: 4923–4931.

41 Chenal J, Pellerin L. Noradrenaline enhances the expression of the neuronal monocarboxylate transporter MCT2 by translational activation via stimulation of PI3K/Akt and the mTOR/S6K pathway. *J Neurochem* 2007; **102**: 389–397.